

Journal Pre-proof

Fabrication of hybrid composite T-Joints by Co-Curing with 3d printed dual cure epoxy

Vera Dahmen, Alec J. Redmann, Johannes Austermann, Adam L. Quintanilla, Sue J. Mecham, Tim A. Osswald



PII: S1359-8368(19)33569-3

DOI: <https://doi.org/10.1016/j.compositesb.2019.107728>

Reference: JCOMB 107728

To appear in: *Composites Part B*

Received Date: 27 June 2019

Revised Date: 5 December 2019

Accepted Date: 16 December 2019

Please cite this article as: Dahmen V, Redmann AJ, Austermann J, Quintanilla AL, Mecham SJ, Osswald TA, Fabrication of hybrid composite T-Joints by Co-Curing with 3d printed dual cure epoxy, *Composites Part B* (2020), doi: <https://doi.org/10.1016/j.compositesb.2019.107728>.

This is a PDF file of an article that has undergone enhancements after acceptance, such as the addition of a cover page and metadata, and formatting for readability, but it is not yet the definitive version of record. This version will undergo additional copyediting, typesetting and review before it is published in its final form, but we are providing this version to give early visibility of the article. Please note that, during the production process, errors may be discovered which could affect the content, and all legal disclaimers that apply to the journal pertain.

© 2019 Published by Elsevier Ltd.

Vera Dahmen: Conceptualization, Methodology, Formal Analysis, Investigation, Writing – Original Draft

Alec J. Redmann: Conceptualization, Methodology, Formal Analysis, Investigation, Writing – Original Draft

Johannes Austermann: Investigation, Writing – Review & Editing

Adam L. Quintanilla: Methodology, Investigation, Writing – Review & Editing

Sue J. Mecham: Methodology, Resources, Writing – Review & Editing, Funding Acquisition

Tim A. Osswald: Conceptualization, Methodology, Writing – Review & Editing, Supervision, Project Administration, Funding Acquisition

FABRICATION OF HYBRID COMPOSITE T-JOINTS BY CO-CURING WITH 3D PRINTED DUAL CURE EPOXY

Vera Dahmen¹, Alec J. Redmann^{1*}, Johannes Austermann¹, Adam L. Quintanilla², Sue J. Mecham², Tim A. Osswald¹

1- Polymer Engineering Center, Department of Mechanical Engineering, University of Wisconsin-Madison, Madison, WI 53706

2- Department of Chemistry, University of North Carolina at Chapel Hill, Chapel Hill, NC 27599

ABSTRACT

A 3D printed dual cure epoxy is evaluated as a bonding material for composite T-joint structures and compared with other traditional bonding materials by mechanical testing. The epoxy is processed in two steps. First, it is 3D printed using Digital Light Synthesis (DLS), a vat photopolymerization process, resulting in semi-rigid, but only partially cured part. This part is then integrated with pre-impregnated fiber reinforced epoxy resin sheets and co-cured in a second, thermally activated, stage.

The bonding strength of the 3D printed epoxy is first investigated by single lap-shear joints and is then implemented in the manufacturing of composite T-joints. The T-joints utilizing 3D printed epoxy as a bonding material show sufficient joint strength in tensile pull-out tests when compared to other common bonding methods. In addition, the 3D printed joints provide a highly reproducible, defect-free bond with improved geometric accuracy. This technology enables the ability to manufacture hybrid composite structures with decreased manufacturing costs due to fewer fixtures, shorter manufacturing times, and a reduction in defects. Furthermore, these adhesive parts can utilize the design freedom of 3D printing by including intricate internal geometries, such as lattice structures, textures, or channels.

Keywords: Hybrid Design, T-joint, Additive Manufacturing, Digital Light Synthesis, Co-curing

1. INTRODUCTION

Fiber reinforced plastics (FRPs) have excellent mechanical properties, however, their design freedom is often limited due to tooling and process conditions. Despite these challenges, the demand for hybrid design with high complexity and a flexible product spectrum for the manufacturing industry is increasing [1]. The application of composite structures is expanding from classical load-bearing structures to complex, multifunctional components with tailored integrated functionality, such as flow channels or lattice structures [2–4]. In order to create such structures, it is necessary to join several smaller components by either mechanical fasteners or adhesive bonding [5]. Both bonding techniques are schematically depicted in Figure 1 for a FRP single lap joint (SLJ).

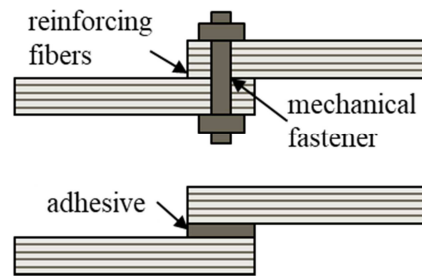


Figure 1: Schematic cross section of single lap joint with mechanical fastening (top) and adhesive bonding (bottom) in FRP.

In general, joining FRP structures with conventional mechanical fasteners is avoided when possible, as they increase the weight and sever the reinforcing fibers, which evokes stress concentrations and decreases the load transfer capabilities [6–8]. Furthermore, mechanical fasteners add significant weight compared to a lightweight adhesive polymer. An adhesive joint in lightweight FRP structures is generally preferred, as it better transfers load in tension and shear across the entire joint, resulting in improved stress distribution and overall joint performance [9].

Figure 2 depicts three common manufacturing processes for joining composite components with different combinations of cured and uncured adherends. The secondary bonding procedure bonds two fully cured adherends and is usually applied for accessible structures with simple geometries. In the co-bonding process, a cured adherend is combined with an initially uncured adherend, which is further co-cured with the adhesive during processing. This method is commonly applied for multi-material structures - for instance when a FRP is bonded with a metal [10]. Finally, co-curing allows the two un-cured adherends to cure simultaneously in a single cycle [11].

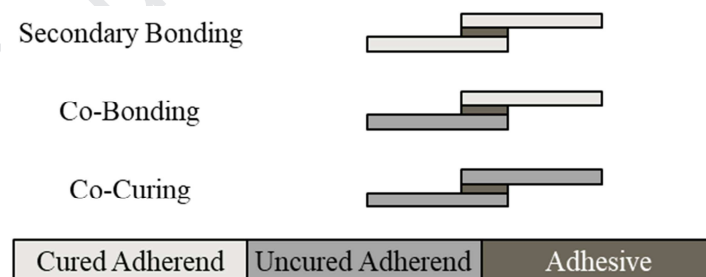


Figure 2: Schematic drawing of common manufacturing processes to join composite components with an adhesive bond

Adhesive bonds are particularly important for the aerospace industry, which is constantly being challenged to enhance airframe structures, as they amount to a large fraction of the total weight and cost of an airplane [12]. The structural adhesive most commonly used for airframe structures is epoxy resin due to its durability, wide temperature ranges and ability to adhere to most surfaces, including aluminum and composites. Other types of adhesives used include silicones or urethanes. [13]

One structural aerospace application, the T-joint, is extensively used for spar-wingskin joints in aircraft wings, which transfers out-of-plane loads for applications with integrated stiffeners [7,14,15]. An example of this is shown in Figure 3. Within the T-joint structure there are several components. The first component, the primary horizontal structure, is referred to as the platform. The vertical internal structure, or web, consists of two bent components to provide an interface which is over-laminated onto the platform. Last, the so-called “deltoid” is the area between the platform and the bent part of the web-components. When the deltoid is filled with a suitable material, it primarily supports the overlaminates, ensuring continuity in the load transfer between the perpendicular components. As the deltoid stabilizes the primary load-bearing plies, the overall strength of the joint is increased [14,16]. Previous literature has shown the strength of specimens with structural deltoid filling was 20% higher compared to the specimens without deltoid filling [17].

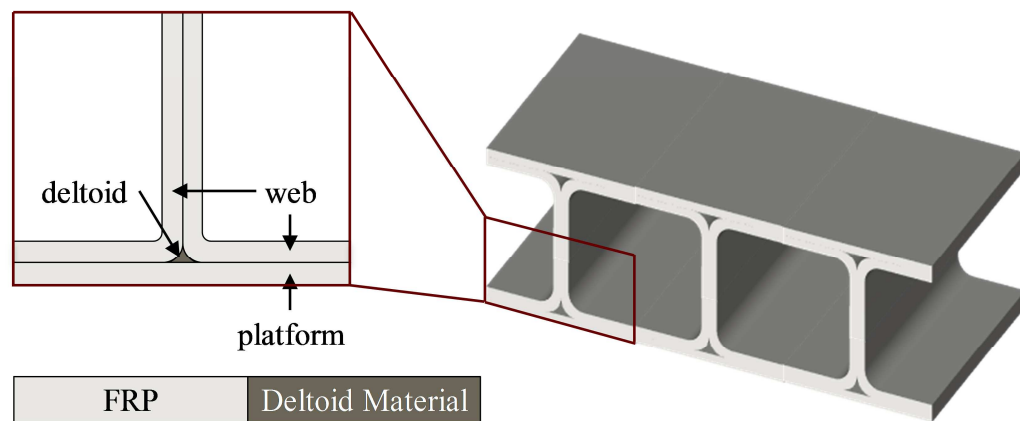


Figure 3: Schematic cross-section of a T-joint (left) and schematic 3D drawing of a spar-wingskin joint (right)

In standard T-joint manufacturing processes, commercial adhesives or rolled-up pre-impregnated reinforcement material are applied in the deltoid area [12,14,18,19]. However, due to the geometry of the deltoid, combined with the manual application and the time sensitivity of the adhesive, it is difficult to ensure uniform surface wetting and geometrical accuracy [12,17]. The insert may need to be formed using custom molds and fixtures before application, which results in a multi-step process. As there are varying deltoid sizes and geometries (e.g. triangular, circular, elliptical), that are commonly applied, this impacts the reproducibility and precision of the bond line, and process times and manufacturing costs are increased [12,14]. In order to solve this problem, there is a need for geometrically tailored bonding materials that improve manufacturing speed, joint reproducibility, and joint strength.

Additive manufacturing (AM), often referred to as 3D printing (3DP), is well suited to produce parts with complex shapes and geometries [20]. When creating hybrid composite structures with 3DP parts, a structure with geometric complexity and specific properties can be achieved. In order to fully utilize a 3DP part as a bonding element in load-bearing structures, it needs to fulfill two requirements: isotropic mechanical properties and chemical potential after the 3DP process.

The chemical potential is particularly important to ensure a uniform adhesive bond with the FRP. However, 3DP parts are usually fully cured after their manufacturing [21].

Digital Light Synthesis (DLS) is an AM technology driven by the Continuous Liquid Interface Production (CLIP) process developed by Carbon, Inc. (Redwood, CA). DLS uses an ultraviolet light source directed through an oxygen-permeable window to continuously and additively generate layers, leading to a part with excellent surface properties and nearly isotropic mechanical behavior [22,23]. The UV curing of DLS creates a rigid part with stable dimensions. However, when a Carbon dual cure resin such as the EPX epoxy-based resin is used, the printed parts are only partially cured. This first stage of the dual cure epoxy system has chemical potential to form an adhesive bond. In the secondary, thermally activated stage, the parts are fully cured [23,24]. The two-stage curing process is shown in Figure 4.

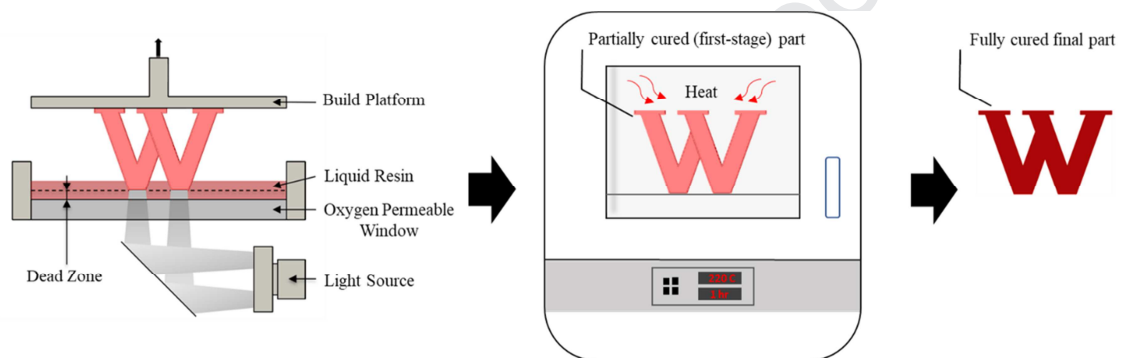


Figure 4: Schematic diagram showing the UV and heat activated curing stages of DLS

Utilizing the DLS process and a dual cure epoxy provides the opportunity to adhesively bond AM parts with FRP structures. The printed parts in their first curing stage can easily be integrated with pre-impregnated fiber reinforcement and the hybrid structure can be co-cured together during the thermal cycle.

The work presented here investigates the suitability of dual cure epoxy manufactured by DLS as bonding material for composite structures. The joints co-cured with the dual cure epoxy are compared to joints manufactured with conventional bonding materials. Single lap-shear joints and T-joints are assessed in terms of manufacturability and joint strength, which is determined by visual bond line inspection and tensile testing, respectively. Figure 5 depicts the design of experiments with the three bonding materials included in this investigation: Dual cure epoxy, epoxy adhesive, and pre-impregnated fiber reinforcement (prepreg).

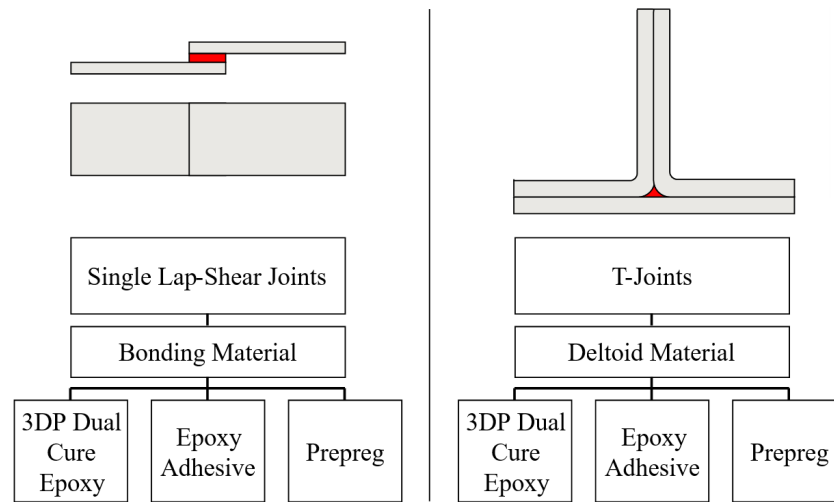


Figure 5: Joint geometries and design of experiments to assess the mechanical properties of different structures and bonding materials

2. EXPERIMENTAL METHODS

2.1 Materials

The tested adherends were manufactured with woven epoxy resin prepreg NB4030-D, by Mitsubishi Chemical Carbon Fiber and Composites, Inc. (Irvine, CA). The layer-wise material properties are listed in Table 1 [24]. The specimens were manufactured with three different adhesive materials: the 3D printed dual-cure epoxy, a standard epoxy adhesive, and prepreg. These three materials are tested to enable a comparison of the dual-cure epoxy with the conventional deltoid materials.

Table 1: Material data of NB4030-D pre-impregnated reinforcement [24]

Material Properties	Value	Unit
NB4030-D		
Nominal Ply Thickness	0.3	mm
Tensile Strength	2370	MPa
Glass Transition Temperature	130	°C
Gel Time (at 135 °C)	5 – 8	min

First, the epoxy-based photopolymer resin EPX 81 from Carbon was manufactured with DLS, completing the first stage of curing reaction during the UV printing process. The printed parts were then removed from the build plate, washed per Carbon's recommended solvent wash process, and stored in a dry container free from external heat or light before being fully co-cured with the prepreg materials. Second, a two-component commercially available epoxy, 3M Scotch-Weld DP190, was applied to a separate set of test samples using the manufacturer recommended dispenser and static mixing nozzle. The material properties of EPX 81 and DP190 are listed in Table 2 [25,26]. Third, the NB4030-D reinforcement material used for the adherends

was also used as a control in the same test geometry. The material properties of NB4030-D are listed in Table 1.

Table 2: Material data of adhesive materials [25,26]

Material Properties	Value	Unit
EPX 81		
Density	1.12	g/cm ³
Tensile Strength	88 ± 3	MPa
Elongation at Break	5.2 ± 0.7	%
Heat Deflection Temperature (at 1.82 MPa)	131	°C
DP190		
Density	1.32	g/cm ³
Tensile Strength	24.13	N/mm ²
Glass Transition Temperature	20	°C
Elongation at Break	30	%
Fixture Time	90	min
Full Cure Time	7	days

2.2 Manufacturing: Single Lap-Shear Joints

The single lap-shear joint (SLJ) specimens were manufactured by co-curing the prepreg material with the different bonding materials in three stages.

The first stage of the manufacturing process was the lay-up of the materials on the mold, which can be subdivided into the four steps shown in Figure 6. One adherend structure, consisting of 12 pre-impregnated reinforcement layers, was laid down on an aluminum plate alongside the margin of a mold (1). Another mold was placed on top of the prepreg layers (2) to ensure accurate application of the bonding material (3). The second adherend structure consisting of another 12 layers was placed on top (4).

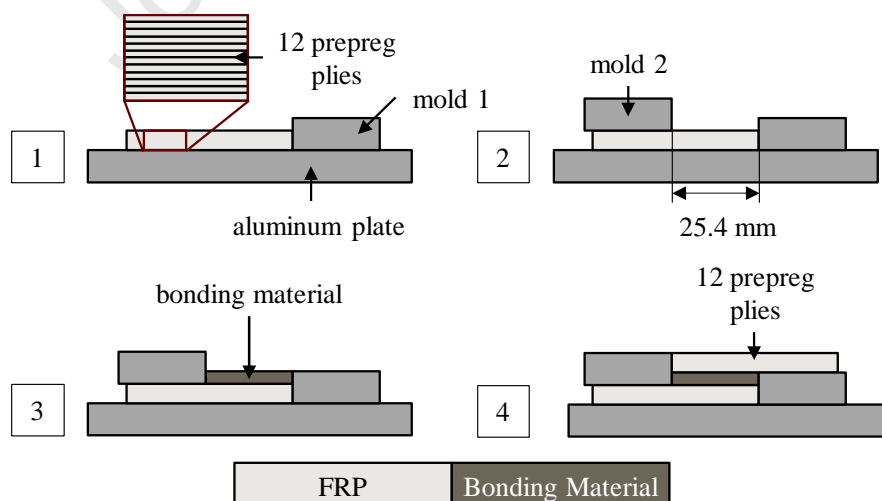


Figure 6: Schematic lay-up process for single lap-shear joints

In a second step, the materials were cured under vacuum in an oven as depicted in Figure 7. With this arrangement, the materials were co-cured according to the temperature cycle for the EPX 81 which is depicted in Figure 8 [25]. For comparability, this temperature cycle is applied for all of the varied bonding materials. Because the curing time and temperature for the prepreg material are lower, it is assumed that the prepreg is fully cured when applying the curing cycle for the EPX 81. [24,26]

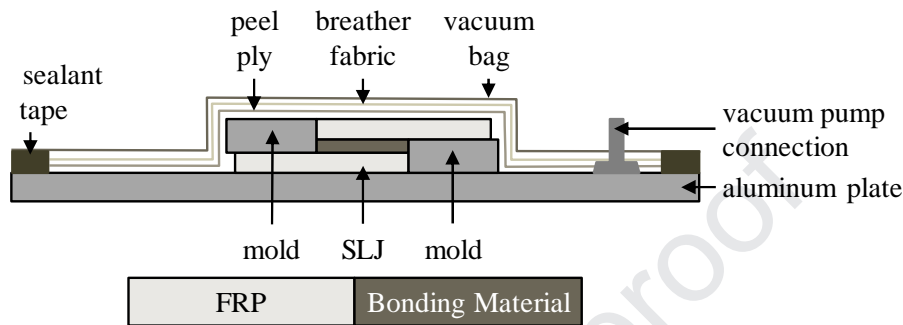


Figure 7: Arrangement of single lap-shear joints for co-curing under vacuum

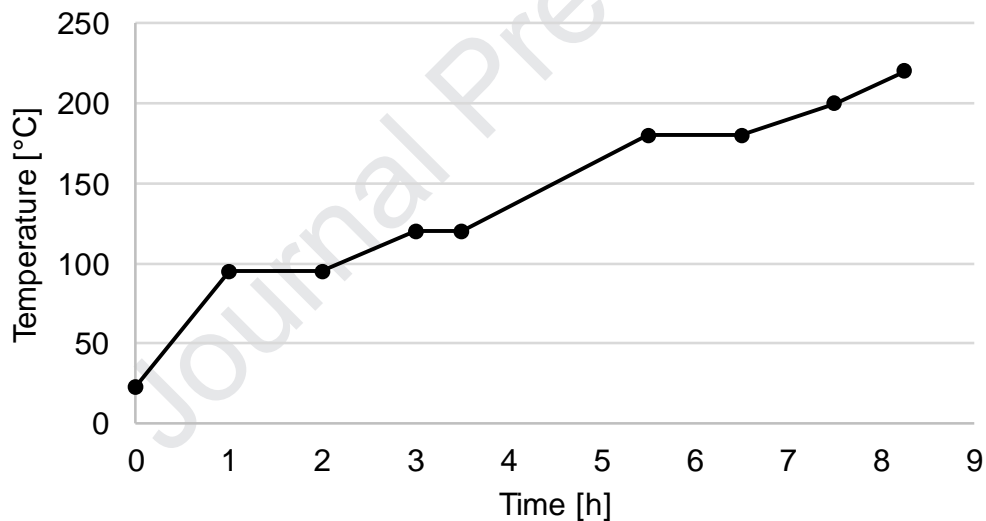


Figure 8: Curing Cycle for Co-Curing of Specimens According to the Curing Cycle for the EPX 81 Epoxy Resin [25]

The specimens were cut to fit the requirements of the tensile testing procedure using a diamond blade wet saw. The specimen geometry, specified in ASTM D5868 [27], is depicted in Figure 9. NEMA Grade G-10 Glass Epoxy Laminate alignment tabs were glued onto the specimens to ensure the centering of the specimens between the tensile testing grips. A finished SLJ specimen is depicted in Figure 10.

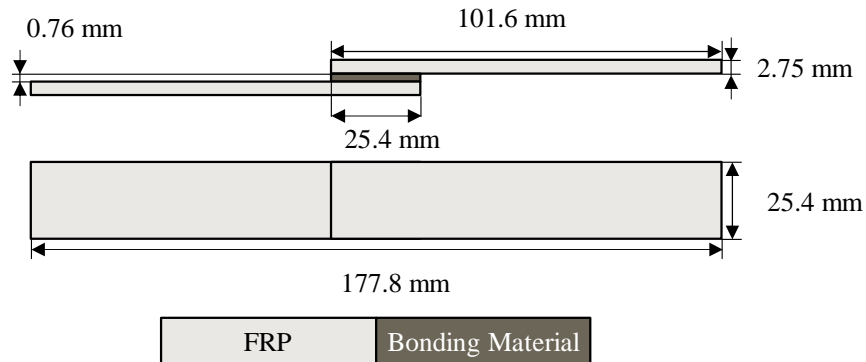


Figure 9: Dimensions for single lap-shear test specimen

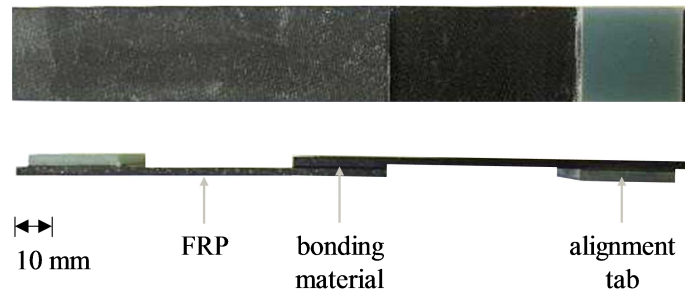


Figure 10: Final manufactured single lap-shear test specimen

2.3 Tensile Testing: Single Lap-Shear Joints

The tensile tests of the lap-shear specimen were performed with a 30 kN load cell on a Instron 5967 universal testing machine from Illinois Tool Works Inc. (Glenview, IL). Following ASTM D5868, the test settings are listed in Table 3 [27]. The maximum force F_{\max} was documented during the testing procedure. Taking the joint surface into account, an approximation of the maximum shear stress τ_{\max} can be derived. The experimental set-up for the tensile testing of the SLJs is depicted in Figure 11. For each bonding material, five specimens were evaluated.

Table 3: Settings of Instron 5967 for tensile testing of lap-shear specimens

Settings	Value	Unit
Load Cell	30	kN
Preload	10	N
Loading Rate	13	mm/min

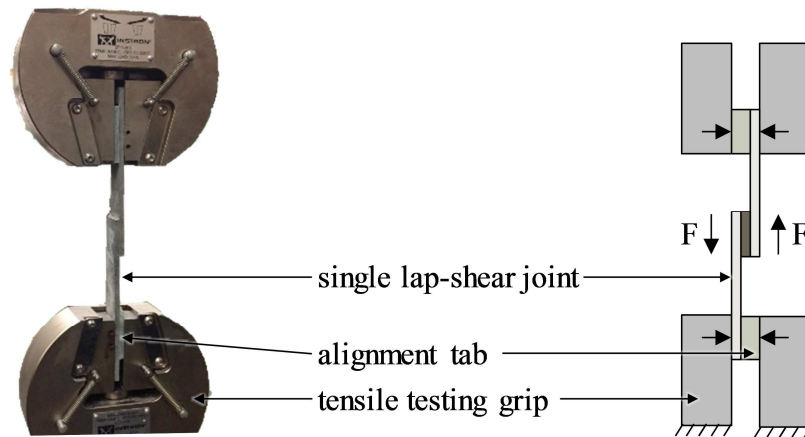


Figure 11: Experimental set-up for tensile testing of single lap-shear joints

2.4 Manufacturing: T-joint Specimens

Currently there are no well-documented standards for the mechanical testing of T-joint specimens. In the following, the manufacturing procedure as well as the tensile testing set-up are adapted from Trask et al. [14] and H el enon et al. [18]. The T-joint specimens were manufactured by co-curing the prepreg material with the varied bonding materials in three steps.

The first step of the manufacturing process is the lay-up, which can be subdivided into four steps as shown in Figure 12. For each half of the web-section, six plies of prepreg material were aligned on two molds, which provide a basis for the geometry of the web-sections (1). Next, the two molds with the laid-up prepreps were aligned against each other (2) and clamped. Subsequently, the specified deltoid insert was placed in the deltoid area (3). When applying the deltoid material, the application varies for the three different materials. First, when applying dual-cure epoxy as deltoid material, the part is simply placed in the deltoid area, as it is manufactured to fit the exact deltoid specifications. When applying the prepreg, the material is cut into long strips, manually rolled into a cylindrical shape, and pressed into a mold to form the deltoid. If the epoxy adhesive is used as deltoid material, it is applied to the deltoid area by means of a static mixing nozzle. Finally, six plies of prepreg were placed for the platform section (4).

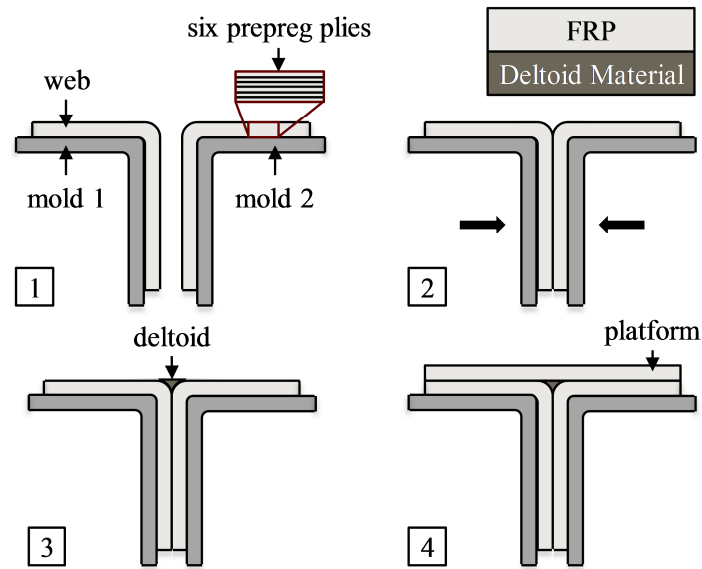


Figure 12: Schematic lay-up process for T-joints

In order to cure the parts, the lay-up was turned over, placed on an aluminum plate and sealed with a vacuum bag, as depicted in Figure 13. Similar to the curing procedure of the SLJ specimens, the materials were co-cured according to the temperature cycle for the EPX 81 [25]. The specimens were cut to fit the requirements of the tensile testing procedure. To ensure accurate geometry and an even surface, the specimens were finished by light sanding. The final dimensions of the T-joint specimens are depicted in Figure 14. A finished T-joint specimen is shown in Figure 15.

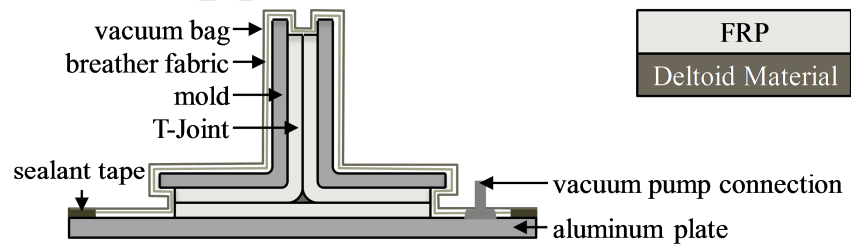


Figure 13: Arrangement of T-joints for co-curing under vacuum

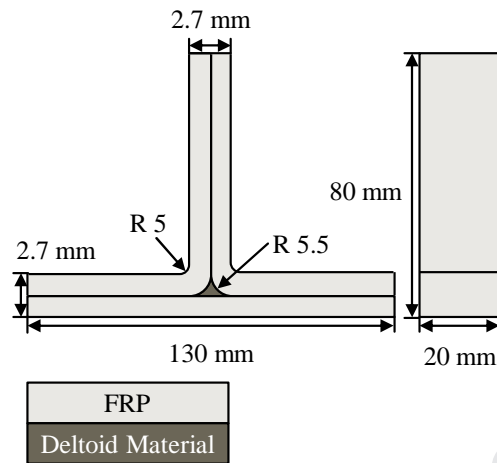


Figure 14: Dimensions of T-joint test specimen

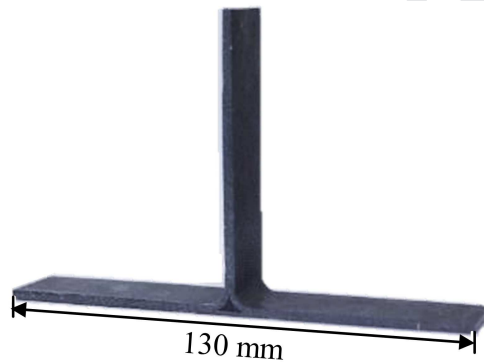


Figure 15: Final manufactured T-joint test specimen

2.5 Tensile Testing: T-Joint Specimens

As previously mentioned, there are no official standards for the mechanical testing of T-joint specimens. The tensile testing set-up and procedure, adapted from Trask et al. [14] and H el enon et al. [18] were adjusted to fit the requirements and boundary conditions for the experiments of this investigation. Analyzing the out-of-plane behavior, a tensile pull-out load was applied to the web-section while the platform-section was braced by pins at both ends. For this experimental set-up, the perpendicular section was clamped with the standard tensile testing fixture. In order to support the horizontal web-section, a customized test fixture was fabricated. The fixture was designed with the purpose to symmetrically support the horizontal section of the T-joint at the designated points. The base of the T-joint is not fixed to the bottom plate to generate a more realistic load case, allowing the horizontal components to bend down [2]. The experimental set-up is shown in Figure 16. For each bonding material, five specimens were evaluated.

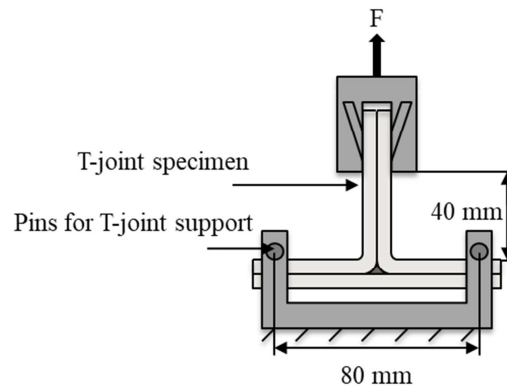


Figure 16: Schematic drawing of experimental set-up with relevant dimensions

The individual T-joint specimens were also tested with a 30 kN load cell on an Instron 5967 universal testing machine from Illinois Tool Works Inc. (Norwood, MA). A tension load was applied to the vertical section at a loading rate of 2 mm/min until joint failure. An initial preload of 5 N was applied to ensure initial contact. Table 4 lists the experimental settings for the tensile tests of the T-joint specimens.

Table 4: Settings of Instron 5967 for tensile testing of T-joint specimens

Settings	Value	Unit
Pin Span	80	mm
Preload	5	N
Loading Rate	2	mm/min

3. RESULTS

3.1 Single Lap-Shear Joints

The maximum shear stresses and standard deviations for the varied bonding materials EPX 81, 3M DP190, and NB4030-D are shown in Figure 17. The results indicate that a suitable bonding strength can be achieved by bonding single lap-shear joints (SLJs) with the EPX 81 when compared to the other traditional bonding methods. The average shear strength of the EPX 81 (7.80 MPa) is slightly higher than the SLJs bonded with prepreg (7.68 MPa). The SLJs utilizing the commercial epoxy adhesive show the highest bonding strength (9.09 MPa).

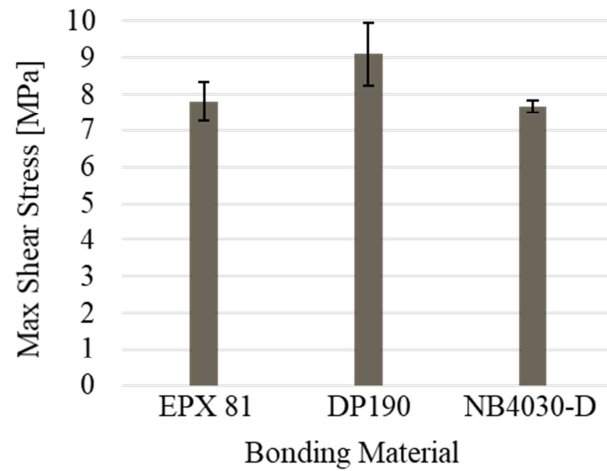


Figure 17: Results of single lap-shear tests with different bonding materials

The differences between the failure modes of the SLJs with varied bonding materials are depicted in Figure 18. The majority of the EPX 81 and DP190 specimens broke with mixed-mode failure with both adhesive and cohesive failure zones observed. The specimens bonded with NB4030-D broke with primarily adhesive failure due to the delamination of the fiber reinforcement. The results indicate that EPX 81 is a suitable bonding material for SLJs and shows adequate bonding qualities for FRP structures.

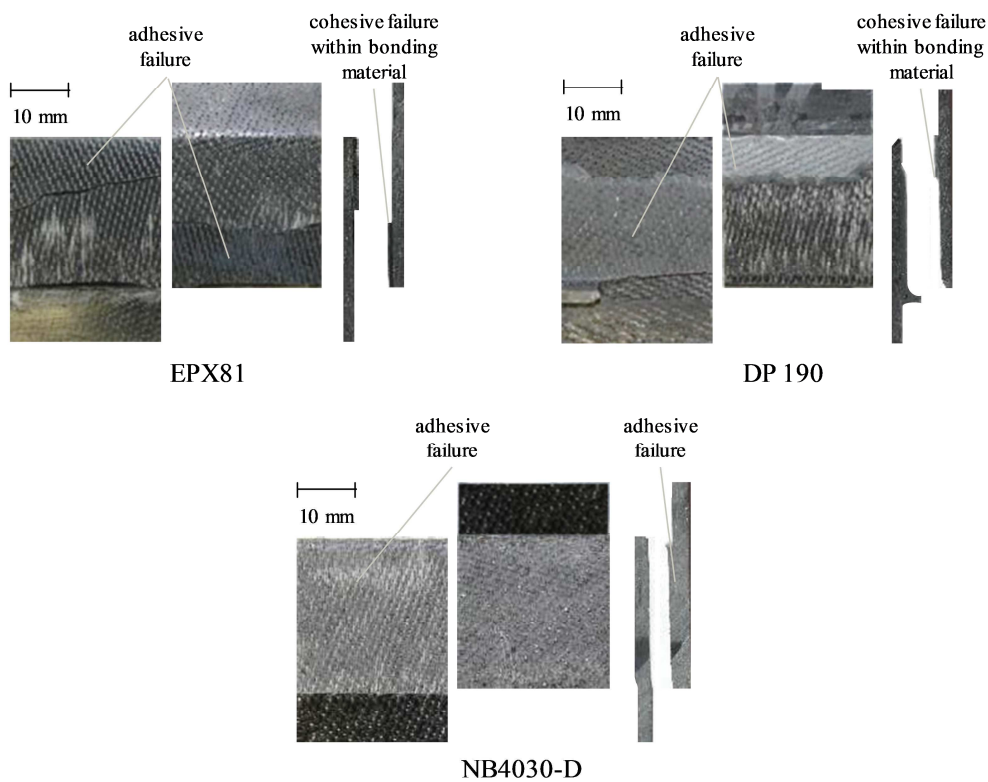


Figure 18: Representative failure modes of single lap-shear joints with varied bonding materials

3.2 T-Joints

Before the T-joint tensile testing was performed, the specimens were visually inspected to evaluate the bond line quality. Figure 19 shows the deltoid areas filled with the three materials. The specimens manufactured with the EPX 81 showed an exact geometry and a good material distribution along the bond line without voids or discontinuities. The specimens manufactured with the commercial epoxy adhesive, however, showed that the material can easily be distributed unevenly within the deltoid area due to insufficient filling during the manual application and/or shrinkage during curing. The T-joint specimens with the prepreg insert generally showed a filled deltoid area and a void-free bond line. However, some specimens show a small defect in the middle of the deltoid, which is possibly induced during manufacturing of the insert where the prepreg is rolled, formed, and placed in the deltoid area manually. None of the defective parts were considered for the subsequent mechanical tests.



Figure 19: Close-up of deltoid areas filled with the different deltoid materials

Figure 20 shows the average load at break and standard deviations for the T-joints with the various deltoid materials. The highest average pull-out joint strength of 418 N was reached by the T-joints with the NB4030-D prepreg as the deltoid inserts. The T-joints that were co-cured with the printed EPX 81 inserts performed nearly the same, with only a 3% reduction in average joint strength of 381 N. The higher standard deviation of the T-joints with the prepreg deltoid inserts may indicate that the quality is susceptible to manufacturing variability. The specimens with the standard DP190 epoxy adhesive showed a significantly lower pull-out joint strength at 284 N.

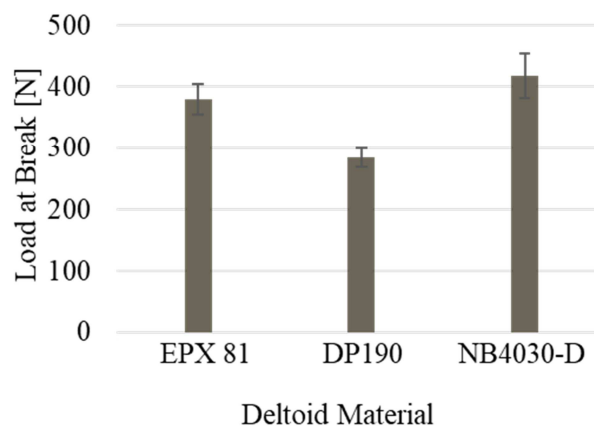


Figure 20: Average load at break for T-joints by deltoid material

From the experimental data it can be concluded that not only the bonding quality has an impact on the results of the mechanical testing, but also the different material properties of the varied bonding/deltoid materials (Table 1 and Table 2). In terms of material properties, the results of the mechanical testing of the T-joints correlate with the data from the SLJs. For example, the commercially available epoxy adhesive DP 190 shows the highest single lap-shear strength, likely due to a high elongation at break. However, the prepreg material EP4030-D performs best in T-joint pull-out testing, likely due to a higher modulus. Thus, it can be concluded that the EPX 81 is well suited for out-of-plane loading conditions due to bond line quality in addition to its material properties.

The failure modes for the different deltoid materials are depicted in Figure 21. The EPX 81 specimens primarily broke by interlaminar failure in the vertical section of the web component. This interlaminar failure propagated to the deltoid section, causing it to crack. In some cases, a bond line failure occurred from the tip of the deltoid along one side. Eventually the bond line failure shifts to a cracking of the deltoid part. The specimens bonded with the commercial DP190 epoxy adhesive experienced interlaminar and bond line failure. The interlaminar failures accumulated around the deltoid region. For the T-joints with NB4030-D prepreg as deltoid material, a bond line failure was observed. This behavior can possibly be traced back to the manufacturing procedure, as the rolled-up deltoid may not accurately fit the deltoid area. As a result, the bond line proves to be a weak point in the joint structure.

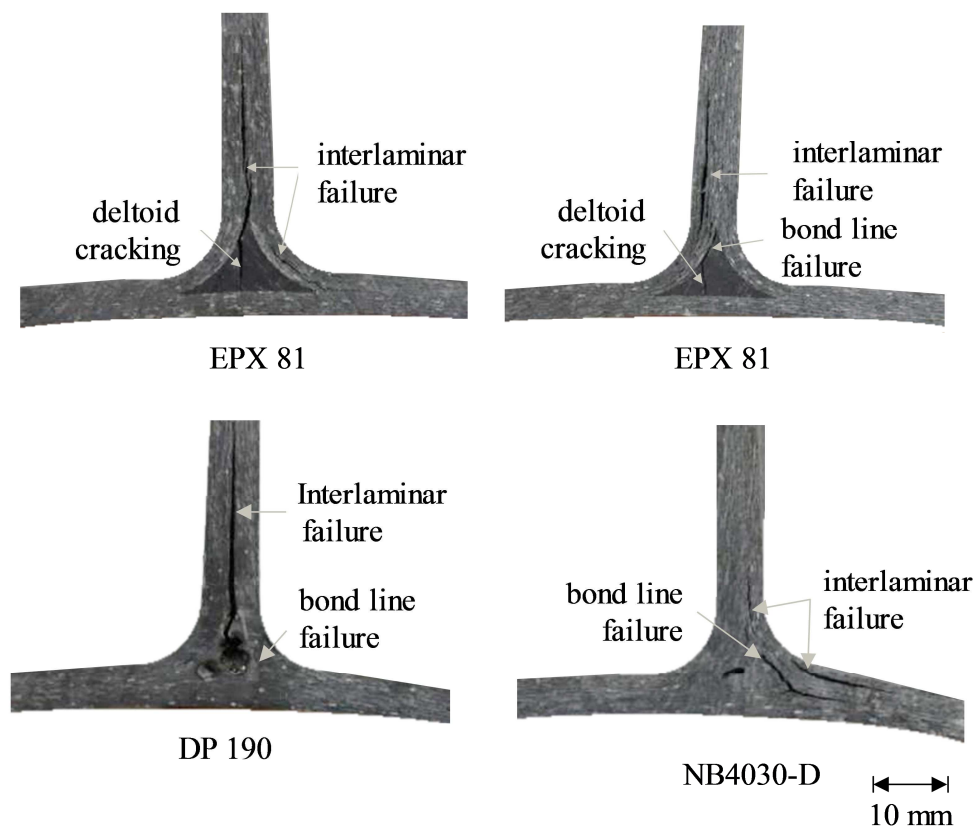


Figure 21: Failure modes of T-joint specimens with varied deltoid material

4. CONCLUSIONS

This paper systematically analyzed the application of Digital Light Synthesis and the dual-cure EPX 81 epoxy for manufacturing hybrid composite T-joint structures. As a proof of concept, the EPX 81 was evaluated in single lap-shear joints and compared to common bonding materials. The highest bonding strength was observed for the single lap-shear joints bonded with the commercial epoxy adhesive. However, the single lap-shear joints bonded with the EPX 81 exhibited shear strengths comparable to the standard NB4030-D prepreg joints while providing a higher reproducibility.

In the investigation of different deltoid materials for T-joints, the 3D printed EPX81 and NB4030-D prepreg material showed the best results as deltoid materials. The DP190 commercial epoxy adhesive had a significantly lower pull-out strength, even though it showed the highest mechanical properties in lap-shear testing. Thus, it can be concluded, that the different bonding materials are suited for different load-cases due to differences in application and material properties.

Furthermore, the specimen manufactured with the EPX 81 showed more exact deltoid geometries as well as improved material distribution along the bond line. Due to precise manufacturing, the reproducibility of the T-joints was highest when using the EPX 81 for the deltoid insert. The results of this paper demonstrate a new technique for manufacturing T-joint structures as well as the potential for manufacturing and hybridization of FRP structures with parts 3D printed by the DLS technology utilizing the advantages of co-curing.

Future investigations should analyze whether DLS as an AM technology enabling high resolution and design freedom can be better utilized in bonding applications. For example, intricate internal geometries could be added, such as lattice structures, textures, or channels. Moreover, the influence of storage time and temperature levels of the dual-cure epoxy after printing should be examined in a future investigation, as the material cures incrementally over time. Furthermore, the co-curing reaction could potentially be improved by better optimization of the thermal cure cycles of the 3D printed bonding resin and the resin used in the pre-impregnated fiber reinforcement.

5. ACKNOWLEDGMENTS

This material is based upon work supported by the National Science Foundation Graduate Research Fellowship Program under Grant No. DGE-1747503. Any opinions, findings, and conclusions or recommendations expressed in this material are those of the authors and do not necessarily reflect the views of the National Science Foundation. Additionally, support was also provided by the Graduate School and the Office of the Vice Chancellor for Research and Graduate Education at the University of Wisconsin-Madison with funding from the Wisconsin Alumni Research Foundation. The authors would like to thank Daniel Miller for the material and design advice. Support for the DLS printing at the University of North Carolina was provided through a sponsored research program with Carbon, Inc. of Redwood City, CA.

Declarations of interest: none

6. REFERENCES

- [1] Kagermann H, Wahlster W, Helbig J. Recommendations for Implementing the Strategic Initiative. Frankfurt Am Main: Industry-Science Research Alliance; 2013.
- [2] Zimmermann K, Zenkert D, Siemetzki M. Testing and Analysis of Ultra Thick Composites. *Compos Part B Eng* 2010;41:326–36. doi:10.1016/j.compositesb.2009.12.004.
- [3] Friedrich HE. *Leichtbau in der Fahrzeugtechnik*. 1st ed. Wiesbaden: Springer Fachmedien Wiesbaden; 2017. doi:10.1007/978-3-658-12295-9.
- [4] Holmström J, Partanen J, Tuomi J, Walter M. Rapid Manufacturing in the Spare Parts Supply Chain. *J Manuf Technol Manag* 2010;21:687–97. doi:10.1108/17410381011063996.
- [5] Junhou P, Sheno RA. Examination of Key Aspects Defining the Performance Characteristics of Out-Of-Plane Joints in FRP Marine Structures. *Compos Part A Appl Sci Manuf* 1996;27A:89–103.
- [6] da Silva LFM, Adams RD. Techniques to Reduce the Peel Stresses in Adhesive Joints with Composites. *Int J Adhes Adhes* 2007;27:227–35. doi:10.1016/j.ijadhadh.2006.04.001.
- [7] Cloud GL, Patterson E, Backman D, editors. *Joining Technologies for Composites and Dissimilar Materials: Proceedings of the 2016 Annual Conference on Experimental and Applied Mechanics*. 10th ed., The Society for Experimental Mechanics, Inc.; 2017.
- [8] Banea MD, da Silva LFM. Adhesively Bonded Joints in Composite Materials: An Overview. *Proc Inst Mech Eng Part L J Mater Des Appl* 2009;223:1–18. doi:10.1243/14644207JMDA219.
- [9] Kinloch AJ. *Adhesion and Adhesives*. 1. Dordrecht: Springer Netherlands; 1987. doi:10.1007/978-94-015-7764-9.
- [10] Molitor P, Young T. Investigations into the use of Excimer Laser Irradiation as a Titanium Alloy Surface Treatment in a Metal to Composite Adhesive Bond. *Int J Adhes Adhes* 2004;24:127–34. doi:10.1016/j.ijadhadh.2003.06.001.
- [11] Budhe S, Banea MD, de Barros S, da Silva LFM. An Updated Review of Adhesively Bonded Joints in Composite Materials. *Int J Adhes Adhes* 2017;72:30–42. doi:10.1016/j.ijadhadh.2016.10.010.
- [12] Panigrahi SK, Pradhan B. Delamination Damage Analyses of FRP Composite Spar Wingskin Joints with Modified Elliptical Adhesive Load Coupler Profile. *Appl Compos Mater* 2008;15:189–205. doi:10.1007/s10443-008-9067-1.
- [13] Mouritz AP. Polymers for aerospace structures. *Introd. to Aersp. Mater.*, Elsevier; 2012, p. 268–302. doi:10.1533/9780857095152.268.
- [14] Trask RS, Hallett SR, Helenon FM, Wisnom MR. Influence of Process Induced Defects on the Failure of Composite T-Joint Specimens. *Compos Part A Appl Sci Manuf* 2012;43:748–57. doi:10.1016/j.compositesa.2011.12.021.
- [15] Flansburg BD, Engelstad SP, Lua J, editors. *Robust Design of Composite Bonded Pi Joints*, American Institute of Aeronautics and Astronautics, Inc.; 2009. doi:10.2514/6.2009-2447.
- [16] Stickler PB, Ramulu M. Investigation of Mechanical Behavior of Transverse Stitched T-Joints with PR520 Resin in Flexure and Tension. *Compos Struct* 2001;52:307–14. doi:10.1016/S0263-8223(01)00023-X.
- [17] Huang CK, Hsu CY. Structural Integrity of Co-Cured Composite Panels. *Mater Manuf*

- Process 2005;20:739–46. doi:10.1081/AMP-200055132.
- [18] Hélénon F, Wisnom MR, Hallett SR, Trask RS. Numerical Investigation into Failure of Laminated Composite T-Piece Specimens under Tensile Loading. *Compos Part A Appl Sci Manuf* 2012;43:1017–27. doi:10.1016/j.compositesa.2012.02.010.
- [19] Cope RD, Pipes BR. Design of the Composite Spar-Wingskin Joint. *Composites* 1982;47–53. doi:10.1016/0010-4361(82)90170-7.
- [20] Türk D-A, Kussmaul R, Zogg M, Klahn C, Leutenecker-Twelsiek B, Meboldt M. Composites Part Production with Additive Manufacturing Technologies. *Procedia CIRP* 2017;66:306–11. doi:10.1016/j.procir.2017.03.359.
- [21] Türk D-A, Triebe L, Meboldt M. Combining Additive Manufacturing with Advanced Composites for Highly Integrated Robotic Structures. *Procedia CIRP* 2016;402–7. doi:10.1016/j.procir.2016.04.202.
- [22] Januszewicz R, Tumbleston JR, Quintanilla AL, Mecham SJ, DeSimone JM. Layerless Fabrication with Continuous Liquid Interface Production. *Proc Natl Acad Sci U S A* 2016;113:11703–8. doi:10.1073/pnas.1605271113.
- [23] Osswald TA. *Understanding Polymer Processing: Processes and Governing Equations*. 2nd ed. Munich and Cincinnati: Hanser Publishers and Hanser Publications; 2017.
- [24] Mitsubishi Chemical Carbon Fiber and Composites. 4030 Data Sheet 2017.
- [25] Carbon Inc. EPX 81 Resin: Biocompatibility Requirements: Printing & Processing Protocols for Carbon M Series Printers 2017.
- [26] 3M Industrial Adhesives and Tapes Division. 3M Scotch-Weld Epoxy Adhesives DP190 Data Sheet 2010.
- [27] ASTM Standard D5868. Test Method for Lap Shear Adhesion for Fiber Reinforced Plastic (FRP) Bonding 2014. doi:10.1520/D5868-01R14.

Author declaration

[Instructions: Please check all applicable boxes and provide additional information as requested.]

1. Conflict of Interest

Potential conflict of interest exists:

We wish to draw the attention of the Editor to the following facts, which may be considered as potential conflicts of interest, and to significant financial contributions to this work:

The nature of potential conflict of interest is described below:

No conflict of interest exists.

We wish to confirm that there are no known conflicts of interest associated with this publication and there has been no significant financial support for this work that could have influenced its outcome.

2. Funding

Funding was received for this work.

All of the sources of funding for the work described in this publication are acknowledged below:

[List funding sources and their role in study design, data analysis, and result interpretation]

NSF Graduate Research Fellowship (DGE-1747503) – Used to fund graduate researcher Alec J. Redmann

Research Program with Carbon, Inc. – Funding provided to the University of North Carolina – Chapel Hill by Carbon, Inc. in the form of their materials used in the 3D printing process

No funding was received for this work.

3. Intellectual Property

We confirm that we have given due consideration to the protection of intellectual property associated with this work and that there are no impediments to publication, including the timing of publication, with respect to intellectual property. In so doing we confirm that we have followed the regulations of our institutions concerning intellectual property.

4. Research Ethics

We further confirm that any aspect of the work covered in this manuscript that has involved human patients has been conducted with the ethical approval of all relevant bodies and that such approvals are acknowledged within the manuscript.

IRB approval was obtained (required for studies and series of 3 or more cases)

Written consent to publish potentially identifying information, such as details or the case and photographs, was obtained from the patient(s) or their legal guardian(s).

5. Authorship

The International Committee of Medical Journal Editors (ICMJE) recommends that authorship be based on the following four criteria:

1. Substantial contributions to the conception or design of the work; or the acquisition, analysis, or interpretation of data for the work; AND
2. Drafting the work or revising it critically for important intellectual content; AND
3. Final approval of the version to be published; AND
4. Agreement to be accountable for all aspects of the work in ensuring that questions related to the accuracy or integrity of any part of the work are appropriately investigated and resolved.

All those designated as authors should meet all four criteria for authorship, and all who meet the four criteria should be identified as authors. For more information on authorship, please see <http://www.icmje.org/recommendations/browse/roles-and-responsibilities/defining-the-role-of-authors-and-contributors.html#two>.

All listed authors meet the ICMJE criteria. ^[I]_[SEP] We attest that all authors contributed

significantly to the creation of this manuscript, each having fulfilled criteria as established by the ICMJE.

One or more listed authors do(es) not meet the ICMJE criteria.

We believe these individuals should be listed as authors because:

[Please elaborate below]

We confirm that the manuscript has been read and approved by all named authors.

We confirm that the order of authors listed in the manuscript has been approved by all named authors.

6. Contact with the Editorial Office

The Corresponding Author declared on the title page of the manuscript is:

Alec Redmann

This author submitted this manuscript using his/her account in EVISE.

We understand that this Corresponding Author is the sole contact for the Editorial process (including EVISE and direct communications with the office). He/she is responsible for communicating with the other authors about progress, submissions of revisions and final approval of proofs.

We confirm that the email address shown below is accessible by the Corresponding Author, is the address to which Corresponding Author's EVISE account is linked, and has been configured to accept email from the editorial office of American Journal of Ophthalmology Case Reports:

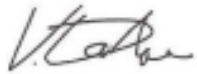
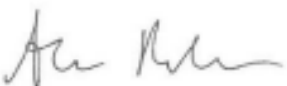




[Insert email address you wish to use for communication with the journal here]

Someone other than the Corresponding Author declared above submitted this manuscript from his/her account in EVISE:

[Insert name below]

We understand that this author is the sole contact for the Editorial process (including EVISE and direct communications with the office). He/she is responsible for communicating with the other authors, including the Corresponding Author, about progress, submissions of revisions and final approval of proofs.

We the undersigned agree with all of the above.

Author's name (Fist, Last)	Signature	Date
1. Vera Dahmen		12/3/2019
2. Alec Redmann		12/3/2019
3. Johannes Austermann		12/3/2019
4. Adam Quintanilla		12/5/2019
5. Sue Mecham		12/4/2019
6. Tim Osswald		12/3/2019